

# Neighboring Optimal Aircraft Guidance in Winds

Matthew R. Jardin\*

NASA Ames Research Center, Moffett Field, California 94035

and

Arthur E. Bryson Jr.†

Stanford University, Stanford, California 94305

The technique of neighboring optimal control is extended to handle cases of parameter change in the system dynamic model. This extension is used to develop an algorithm for optimizing horizontal aircraft trajectories in general wind fields using time-varying linear feedback gains. The minimum-time problem for an airplane traveling horizontally between two points in a variable wind field (a type of Zermelo problem) is used to illustrate how perturbations in system parameters can be accounted for by augmenting the dynamic model with additional bias states. For the special case of a constant wind shear in the cross-track direction, analytical and numerical results are derived for bias perturbations. Numerical simulations are presented to demonstrate the performance of the proposed state-augmentation technique. An additional example is used to demonstrate an algorithm to compute near-optimal trajectories in general wind fields. The algorithm is based on nondimensionalizing the neighboring optimal control solutions and using piecewise linearly varying wind and horizontal wind shear parameters. One proposed application of this technique is to the computation and real-time update of time-optimal trajectories in wind fields by onboard flight management systems and by ground-based air traffic management automation tools.

## Introduction

THE technique of neighboring optimal control (NOC) produces time-varying feedback control that minimizes a performance index to second order for perturbations from a nominal optimal path. Perturbations in the nominally optimal states are compensated for, but errors in the system dynamic model parameters, for example, wind speed or wind shear, may result in substantially suboptimal performance. In this paper, the minimum-time problem for an airplane traveling horizontally between two points in a wind field (a type of Zermelo problem) will be examined to illustrate how perturbations in model parameters can be accounted for by augmenting the dynamic model with additional states. The NOC solution has been derived analytically for the case where the wind field is modeled as a constant wind shear in the cross-track direction.<sup>1,2</sup> This existing NOC solution for the Zermelo problem is extended to cases of bias perturbations in the wind shear parameter. For a more general wind field, piecewise linearly varying perturbations in the wind parameters are introduced to the NOC problem formulation and solution.

Previous work in incorporating bias parameter perturbations in NOC problems has treated parameter perturbations separately from state perturbations, therefore requiring extensions to the backward sweep solution method.<sup>3,4</sup> The current method differs by treating bias parameters as additional system states. By the use of this approach, the NOC problem may be readily solved with the backward sweep method. Another benefit to this approach is that it may be easily extended to dynamically varying parameters.

In the next section, the Zermelo problem will be introduced. Then the NOC technique will be described, followed by a section on the NOC solution to the particular Zermelo problem of computing minimum-time trajectories for an aircraft in different wind shear conditions. The paper concludes with several simulation examples to show how NOC can be applied to achieve minimum-time trajectories in different wind and wind shear conditions. The first two examples

are of a perturbation in a bias wind shear parameter. The last two examples show how more general wind and wind shear fields may be accounted for by incorporating piecewise linearly varying wind and wind shear parameters.

## Zermelo Problem

The classic Zermelo problem is to find minimum-time paths through a region of position-dependent vector velocity.<sup>1,2</sup> Here the system used to illustrate this problem is that of an airplane traveling through a region of varying winds. The equations of motion are given by

$$\dot{x} = V \cos \theta + u(x, y) \quad (1)$$

$$\dot{y} = V \sin \theta + v(x, y) \quad (2)$$

where  $x$  and  $y$  are rectangular coordinates and  $V$  is the airplane velocity relative to the air mass (the airspeed). The  $x$  component of the wind velocity is  $u(x, y)$ , and the  $y$  component is  $v(x, y)$ . The heading angle  $\theta$  is the control available for achieving the minimum-time objective.

An implicit analytical solution has been derived for the case where the  $x$ -direction wind speed varies linearly in the  $y$  direction.<sup>1,2</sup> For  $u(x, y) = -V_{ws}y$  and  $v(x, y) = 0$ , the heading  $\theta$  at the point  $\{x, y\}$  to go to the origin in minimum time is computed implicitly from the following equations:

$$y = (V/V_{ws})(\sec \theta - \sec \theta_f) \quad (3)$$

$$x = (V/2V_{ws})[\operatorname{asinh}(\tan \theta_f) - \operatorname{asinh}(\tan \theta) + \tan \theta(\sec \theta_f - \sec \theta) - \sec \theta_f(\tan \theta_f - \tan \theta)] \quad (4)$$

where the constant wind shear parameter  $V_{ws}$  has been introduced. The time to go is given by

$$T = (1/V_{ws})(\tan \theta_f - \tan \theta) \quad (5)$$

In addition to the inclusion of the  $V/V_{ws}$  terms in these expressions, several minor typographical errors in Refs. 1 and 2 have been corrected in Eqs. (3–5). A specific example of a wind-optimal trajectory will now be shown.

For initial conditions,  $x_0 = 2500$  n mile and  $y_0 = 0$ , an airspeed of  $V = 480$  kn, and a wind shear in the  $y$  direction of  $V_{ws} = 0.2$  kn/n mile, the minimum time to reach the origin as computed with Eqs. (3–5) is  $t_{\min} = 300.4$  min (Fig. 1). The wind shear conditions used in this example are representative of what might be experienced by a westbound flight across the United States.

Received 26 June 2000; revision received 10 November 2000; accepted for publication 30 November 2000. Copyright © 2001 by the American Institute of Aeronautics and Astronautics, Inc. No copyright is asserted in the United States under Title 17, U.S. Code. The U.S. Government has a royalty-free license to exercise all rights under the copyright claimed herein for Governmental purposes. All other rights are reserved by the copyright owner.

\*Electronics Engineer, Automation Concepts Research Branch, MS 210-10. Member AIAA.

†Pigott Professor of Engineering Emeritus, Department of Aeronautics and Astronautics. Honorary Fellow AIAA.

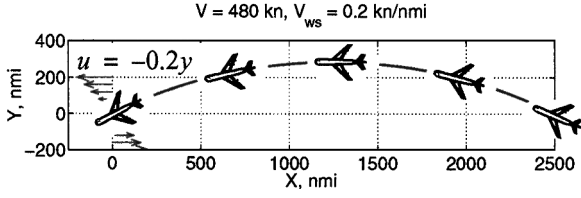


Fig. 1 Minimum-time path for an airplane in a constant wind shear.

### NOC

NOC is a time-varying linear feedback control algorithm that minimizes a performance index to second order.<sup>1,2</sup> NOC regulators are very similar to the more common linear quadratic regulator (LQR). In LQR design, the control engineer adjusts terms in the cost function,  $J$ , weighting matrices,  $Q$ ,  $R$  and  $N$ , to achieve good regulator performance:

$$J = \int_0^\infty \left( [\Delta \bar{x}^T \quad \Delta \bar{u}^T] \begin{bmatrix} Q & N \\ N^T & R \end{bmatrix} \begin{bmatrix} \Delta \bar{x} \\ \Delta \bar{u} \end{bmatrix} \right) dt \quad (6)$$

The difference with NOC is that the weighting matrices are elements of the Hessian matrix of an optimizing cost function as follows:

$$J = \int_0^{t_f} \left( [\Delta \bar{x}^T \quad \Delta \bar{u}^T] \begin{bmatrix} H_{xx} & H_{xu} \\ H_{ux} & H_{uu} \end{bmatrix} \begin{bmatrix} \Delta \bar{x} \\ \Delta \bar{u} \end{bmatrix} \right) dt \quad (7)$$

where  $H$  is the Hamiltonian of the dynamic system being optimized and the subscript  $x$  and  $u$  denote partial differentiation with respect to the states and controls. In NOC, the feedback gains may be tabulated as functions of time to go, and the perturbation in the final time may be estimated so that an NOC controller can be used to achieve minimum-time solutions. This is a feature that is not possible with the LQR.

The details of computing NOC controllers are lengthy and are treated in Refs. 1 and 2. The important point about NOC is that it is a linear feedback algorithm where, for systems with fixed final conditions, the perturbation controller has the following form:

$$\delta \bar{u}(T) = -K_{ux}(T) \delta \bar{x}(T) \quad (8)$$

where  $\delta \bar{u}(T)$  is the perturbation from the nominal control vector,  $\delta \bar{x}(T)$  is the perturbation from the nominal state vector,  $K_{ux}(T)$  is the neighboring optimal feedback gain matrix, and  $T$  is the time to go on the nominal optimal path. The appropriate nominal states, controls, and feedback gains are selected based on finding the same time to go on the actual path and the nominal path by using the following NOC feedback relation to update the optimal final time  $t_f$ :

$$dt_f = -K_{tx}(T) \delta \bar{x}(T) \quad (9)$$

When a system has small perturbations, neighboring optimal controls are generated by feedforward of the nominal optimal controls and linear feedback of perturbations from the nominal optimal state trajectory (Fig. 2). This should not be mistaken for simply regulating a system to follow a nominal trajectory. Use of the neighboring optimal regulator gains will minimize the original cost function to second order.

For most problems, nominal optimal solutions and NOC feedback gains must be computed numerically because complexity precludes analytical solutions. The numerical solution method used to generate the NOC gains in the sections that follow was the backward sweep method with unspecified final time. The required first and second derivatives of the dynamic system equations were derived analytically and coded into MATLAB<sup>®</sup> routines for numerical solution of the backward sweep equations to produce tables of NOC gains vs time to go. The nominal optimal trajectories have been computed to within the following numerical optimization tolerances:

$$\begin{aligned} \delta \theta &\leq 1 \times 10^{-5} \text{ rad}, & (\|[\delta x_f \quad \delta y_f]\|/\sqrt{2}) &\leq 2.5 \times 10^{-3} \text{ n mile} \\ |\delta t_f| &\leq 0.01875 \text{ s} \end{aligned}$$

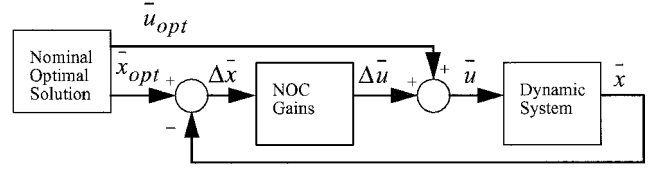


Fig. 2 Block-diagram of NOC.

### NOC Solution to the Zermelo Problem

The NOC solution for the Zermelo problem with a constant cross-track wind shear has been computed both numerically and analytically and is presented in Ref. 2. The resulting analytical feedback gains are repeated here with some minor corrections to typographical errors and to show how the numerical results for this problem have been verified.

The perturbation feedback laws for  $\theta$  and  $\theta_f$  are given by

$$\begin{bmatrix} \delta \theta \\ \delta \theta_f \end{bmatrix} = \begin{bmatrix} \frac{\partial \theta}{\partial x} & \frac{\partial \theta}{\partial y} \\ \frac{\partial \theta_f}{\partial x} & \frac{\partial \theta_f}{\partial y} \end{bmatrix} \begin{bmatrix} \delta x \\ \delta y \end{bmatrix} \quad (10)$$

where the perturbation of any variable,  $A$ , is defined by  $\delta(A) \equiv (A - A_{\text{nominal}})$ , and the partial derivatives of  $\theta$  and  $\theta_f$  are given by

$$\frac{\partial \theta}{\partial x} = \left( \frac{1}{D} \right) \frac{\partial y}{\partial \theta_f} \quad (11)$$

$$\frac{\partial \theta}{\partial y} = \left( \frac{-1}{D} \right) \frac{\partial x}{\partial \theta_f} \quad (12)$$

$$\frac{\partial \theta_f}{\partial x} = \left( \frac{-1}{D} \right) \frac{\partial y}{\partial \theta} \quad (13)$$

$$\frac{\partial \theta_f}{\partial y} \equiv \left( \frac{1}{D} \right) \frac{\partial x}{\partial \theta} \quad (14)$$

and the common denominator term  $D$  is given by

$$D = \frac{\partial x}{\partial \theta} \cdot \frac{\partial y}{\partial \theta_f} - \frac{\partial x}{\partial \theta_f} \cdot \frac{\partial y}{\partial \theta} \quad (15)$$

The partial derivatives of  $x$  and  $y$  with respect to  $\theta$  and  $\theta_f$  are given by

$$\frac{\partial x}{\partial \theta} = \frac{V[2 \sec^2 \theta (\sec \theta_f - \sec \theta) + \sec \theta - |\sec \theta|]}{2 V_{ws}} \quad (16)$$

$$\frac{\partial y}{\partial \theta} = \frac{V}{V_{ws}} \sec \theta \tan \theta \quad (17)$$

$$\frac{\partial x}{\partial \theta_f} = \frac{1}{2} \frac{V}{V_{ws}} [2 \sec \theta_f (\tan \theta_f \tan \theta - \sec^2 \theta_f) + \sec \theta_f + |\sec \theta_f|] \quad (18)$$

$$\frac{\partial y}{\partial \theta_f} = -\frac{V}{V_{ws}} \sec \theta_f \tan \theta_f \quad (19)$$

The total heading command is then given by

$$\theta(T) = \theta_{\text{nom}}(T) + \frac{\partial}{\partial x} \theta(T) \delta x(T) + \frac{\partial}{\partial y} \theta(T) \delta y(T) \quad (20)$$

The reference point is determined by the point with the same time to go as the point on the nominal path. Differential changes in  $T$  are given by

$$\begin{aligned} dT &= \frac{\partial T}{\partial x} \delta x + \frac{\partial T}{\partial y} \delta y = \left( \frac{\partial T}{\partial \theta} \cdot \frac{\partial \theta}{\partial x} + \frac{\partial T}{\partial \theta_f} \cdot \frac{\partial \theta_f}{\partial x} \right) \delta x \\ &\quad + \left( \frac{\partial T}{\partial \theta} \cdot \frac{\partial \theta}{\partial y} + \frac{\partial T}{\partial \theta_f} \cdot \frac{\partial \theta_f}{\partial y} \right) \delta y \end{aligned} \quad (21)$$

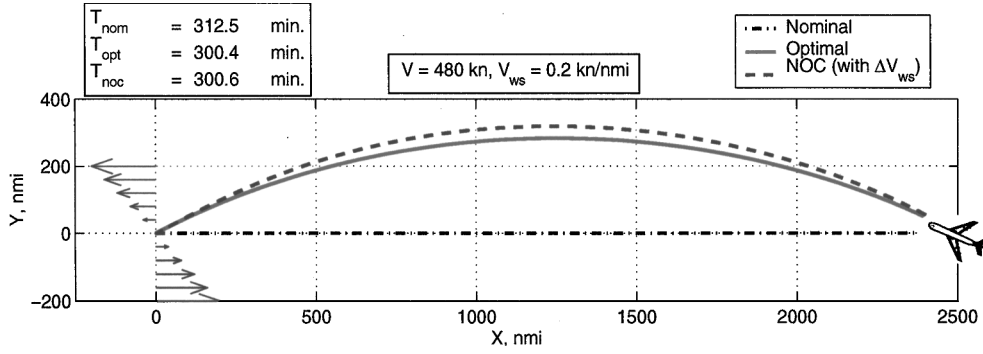


Fig. 3 Neighboring optimal solution computed around a nominal trajectory with zero wind shear is nearly identical to the optimal solution.

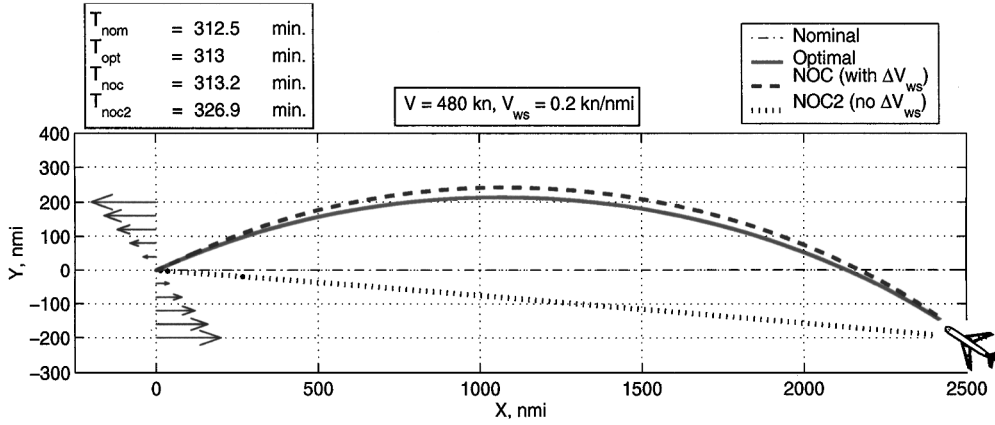


Fig. 4 Simulation with both an initial position perturbation and a perturbation in the wind shear parameter.

where

$$\frac{\partial T}{\partial \theta} = -\frac{\sec^2 \theta}{V_{ws}} \quad (22)$$

$$\frac{\partial T}{\partial \theta_f} = \frac{\sec^2 \theta_f}{V_{ws}} \quad (23)$$

When given the current coordinates  $\{x, y\}$ , we find the appropriate value of  $T$  by solving Eq. (21) for  $dT=0$ . By doing so, we are determining the location on the actual path with the same time to go as the corresponding point on the nominal path. With this value of  $T$ , we obtain the appropriate values of the feedback gains and nominal controls from lookup tables.

### Perturbations in Cross-Track Wind Shear

To allow for a perturbation in the cross-track wind shear parameter  $V_{ws}$ , the system dynamic model [Eqs. (1) and (2) with  $u(x, y) = -V_{ws}y$  and  $v(x, y) = 0$ ] is augmented with the following state:

$$\dot{V}_{ws} = 0 \quad (24)$$

Note that Eq. (24) could easily be replaced with any other appropriate dynamic model, for example, an exponential decay process, if so desired.

If the nominal optimal controls are computed for a nominal value of  $V_{ws}$ , we can then generate neighboring optimal controls for different conditions as measured during the airplane's travel.

To demonstrate the effect of incorporating the bias state model for  $V_{ws}$ , a simulation has been performed for a case where no a priori information about the value of the wind shear parameter is assumed during the computation of the nominal trajectory and NOC gains. In this case, the nominal optimal trajectory and NOC gains are computed for  $V_{ws} = 0$ . The resulting nominal optimal trajectory is simply a straight line from the initial point  $\{2500 \text{ n mile}, 0\}$  to the origin, and the nominal minimum time is 312.5 min. The NOC feedback simulation is performed for the case where the actual wind shear

parameter is measured just before the flight to be  $V_{ws} = 0.2 \text{ kn/n mile}$  (the same as shown in Fig. 1).

The resulting NOC trajectory is nearly identical to the optimal trajectory for these wind shear conditions (Fig. 3). The reduction in time due to taking advantage of the wind shear is about 12 min, or 4% of the optimal flight time. Without including the wind shear feedback terms in the simulation, the resulting trajectory is indistinguishable from the nominal trajectory. To further highlight the importance of including information about perturbations in the wind shear, a second NOC simulation was performed with perturbations in both the initial position and the wind shear (Fig. 4). The resulting trajectories and final times clearly demonstrate the benefit to be gained by including wind shear feedback. The reduction in flight time due to the inclusion of wind shear feedback as opposed to not using wind shear feedback is about 13.7 min, or 4.4% of the optimal flight time.

To verify the numerical results, the analytical solution has also been computed for this case. The derivation is very similar to the one shown earlier in Eqs. (10–23) and will only be outlined here. Perturbations in  $\theta$  and  $\theta_f$  may be computed as functions of perturbations in  $x, y$ , and now  $V_{ws}$  as shown in the following equation:

$$\begin{bmatrix} \delta \theta \\ \delta \theta_f \end{bmatrix} = \begin{bmatrix} \frac{\partial \theta}{\partial x} & \frac{\partial \theta}{\partial y} & \frac{\partial \theta}{\partial V_{ws}} \\ \frac{\partial \theta_f}{\partial x} & \frac{\partial \theta_f}{\partial y} & \frac{\partial \theta_f}{\partial V_{ws}} \end{bmatrix} \begin{bmatrix} \delta x \\ \delta y \\ \delta V_{ws} \end{bmatrix} \quad (25)$$

and the time-to-go perturbation is given by

$$\delta T = \frac{\partial T}{\partial x} \delta x + \frac{\partial T}{\partial y} \delta y + \left( \frac{\partial T}{\partial V_{ws}} + \frac{\partial T}{\partial \theta} \frac{\partial \theta}{\partial V_{ws}} + \frac{\partial T}{\partial \theta_f} \frac{\partial \theta_f}{\partial V_{ws}} \right) \delta V_{ws} \quad (26)$$

where

$$\frac{\partial \theta}{\partial V_{ws}} \equiv - \left( \frac{\partial \theta}{\partial x} \frac{\partial x}{\partial V_{ws}} + \frac{\partial \theta}{\partial y} \frac{\partial y}{\partial V_{ws}} \right) \quad (27)$$

$$\frac{\partial \theta_f}{\partial V_{ws}} \equiv - \left( \frac{\partial \theta_f}{\partial x} \frac{\partial x}{\partial V_{ws}} + \frac{\partial \theta_f}{\partial y} \frac{\partial y}{\partial V_{ws}} \right) \quad (28)$$

The remaining partial derivatives in Eqs. (25–28) are straightforward to compute from the expressions for  $x$ ,  $y$ , and  $T$  in Eqs. (3–5), and the numerically computed neighboring optimal feedback gains have been verified with the resulting analytical values.

### Minimum-Time Paths Through a General Wind Field

A practical wind optimization algorithm will now be developed by incorporating piecewise linearly varying along-track ( $x$ -direction) and cross-track ( $y$ -direction) winds. To further improve the utility of the algorithm, the nondimensional form of the equations will be derived. When this is done, a single NOC solution can be applied to a wide range of different flight distances, airspeeds, wind speeds, and wind shears. This similarity property of the solution for changes in wind parameters is only made possible by the state-augmentation procedure presented here.

The winds in a horizontal plane may be modeled very generally by a two-dimensional grid of wind values with piecewise linear interpolation used to determine the values between grid points.<sup>5</sup> Equivalently, a one-dimensional wind model may be developed where the winds at each point are expressed as the sum of a cross-track shear term and a bias wind term. When the second approach is taken, the nondimensional along-track wind component  $\eta_x$  is given by the following expression:

$$\eta_x(\chi, \gamma) = -\eta_{ws}(\chi) \cdot \gamma + \eta_{uw}(\chi) \quad (29)$$

Because any cross-track wind shear in the cross-track wind component would not have a strong effect on the minimum-time trajectory solution, the nondimensional cross-track wind component is simplified to a piecewise linear function of  $\chi$  only

$$\eta_y(\chi, \gamma) = \eta_{vw}(\chi) \quad (30)$$

These nondimensional variables are related to their dimensional counterparts by the following equations:

$$\chi \equiv x/L \quad (31)$$

$$\gamma \equiv y/L \quad (32)$$

$$\eta_{ws}(\chi) \equiv V_{ws}(\chi)(L/V) \quad (33)$$

$$\eta_{uw}(\chi) \equiv u_w(\chi)/V \quad (34)$$

$$\eta_{vw}(\chi) \equiv v_w(\chi)/V \quad (35)$$

where  $V$  is the airspeed,  $L$  is the nominal straight-line distance between the initial and final coordinate points, and  $\{u_w, v_w\}$  are the  $x$  and  $y$  components of the wind vector.

The piecewise linear functions of  $\chi$ ,  $[\eta_{ws}(\chi), \eta_{uw}(\chi), \eta_{vw}(\chi)]$  may be written in the following way:

$$\eta(\chi) = \eta_i + (\eta_{i+1} - \eta_i)[(N_\eta - 1)\chi - (i - 1)]$$

$$(i - 1)/(N_\eta - 1) \leq \chi < i/(N_\eta - 1), \quad i = 1, 2, \dots, (N_\eta - 1) \quad (36)$$

where the  $\eta_i$  are the function values at the locations  $\chi = (i - 1)/(N_\eta - 1)$  and  $N_\eta$  are the number of grid locations for any parameter  $\eta$ .

In nondimensional form, the dynamic equations for the Zermelo problem with the given wind model are given by

$$\chi' = \cos \theta - \eta_{ws}(\chi) \cdot \gamma + \eta_{uw}(\chi) \quad (37)$$

$$\gamma' = \sin \theta + \eta_{vw}(\chi) \quad (38)$$

The prime operator represents differentiation with respect to nondimensional time  $\tau$ , which is related to dimensional time by the following equation:

$$\tau \equiv t(V/L) \quad (39)$$

The dynamic model is then augmented with bias states for each wind and wind shear parameter at each grid location,

$$\eta'_{wsi} = 0, \quad i = 0, 1, 2, \dots, N_{ws} \quad (40)$$

$$\eta'_{uwi} = 0, \quad i = 0, 1, 2, \dots, N_{uw} \quad (41)$$

$$\eta'_{vwi} = 0, \quad i = 0, 1, 2, \dots, N_{vw} \quad (42)$$

The major difference in the numerical NOC solution between this and the earlier examples in this paper is that the analytical first and second derivatives of the system equations with respect to the states are now piecewise linear functions of  $\chi$ . A few new derivative terms arise due to the inclusion of bias wind parameters, but the solution to the problem specified in Eqs. (29–42) does not require any special techniques beyond what was used to solve the earlier two simulation examples.

To illustrate the NOC solution for a generalized wind field, some simulation results will now be presented. As in the preceding examples, the airspeed is  $V = 480$  kn, and the range is  $L = 2500$  n mile. The number of piecewise linear wind and wind shear terms has been set to three each. The wind shear perturbation has been chosen to vary from  $V_{ws1} = -0.4$  kn/n mile at the initial trajectory position to  $V_{ws2} = 0$  kn/n mile at the halfway position, and finally to  $V_{ws3} = 0.4$  kn/n mile at the final trajectory position (Fig. 5). The nominal and perturbed values of the bias wind parameters have been chosen based on the average and standard deviation of the

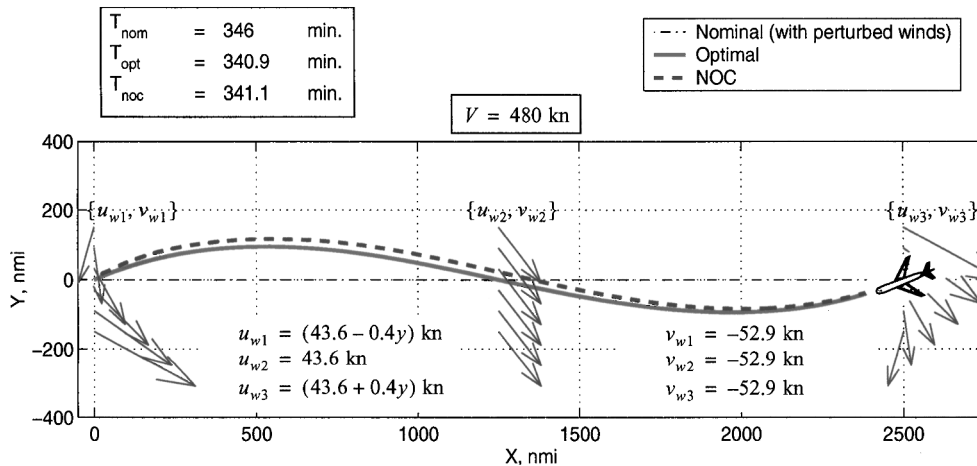


Fig. 5 Simulation with piecewise linear perturbations in wind and wind shear.

wind speed and direction from aircraft data collected between August 1996 and August 1997 in airspace spanning approximately 1000 n mile east to west and roughly coinciding with jet altitudes in the Denver air route traffic control center.<sup>6</sup> These data represent one of the most complete sets of aircraft-reported wind data to be collected over such a large region of airspace and should provide a realistic range of wind speed and direction values on a continental scale. The nominal and perturbed values of the wind and wind shear parameters are given in Table 1. Note that the variation in bias wind conditions between the nominal and perturbed cases chosen for this example is rather severe with the wind vector magnitude increasing by more than 25 kn and the wind direction changing by about 68 deg. Even with these severe perturbations, the NOC solution is remarkably close to the optimal solution (Fig. 5). The final time for the NOC solution is about 5 min less than for a straight-line trajectory in the same perturbed wind field (about 1.4% of the optimal time).

A plot of the shear-perturbation feedback gains vs time to go shows how the NOC solution is able to adapt to perturbation conditions at future positions along the trajectory (Fig. 6). Note that the feedback gain corresponding to wind shear perturbations at the final position  $K_{V_{ws1}}$  is nonzero throughout the trajectory. This shows that a perturbation in the wind shear 2500 n mile away from the initial aircraft position has an effect on the control of the aircraft such that the total time to fly is minimized.

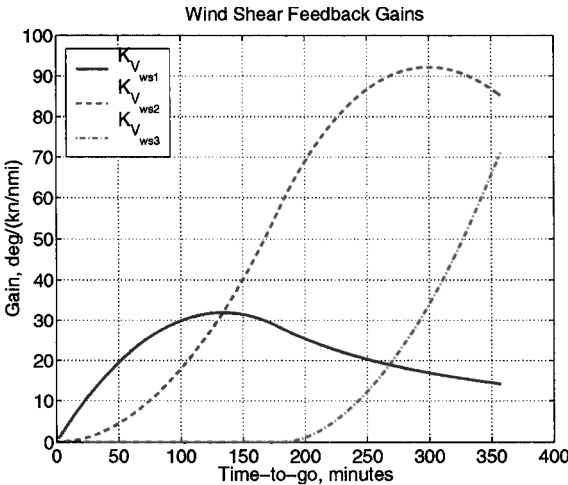


Fig. 6 Wind shear feedback gains show that perturbations in wind shear at future positions affect the entire trajectory.

Because the NOC gains have been computed in nondimensional form, entire families of NOC solutions may be generated for many different airspeeds, flight distances, wind speeds, and wind shears using the same set of feedback gains. To illustrate this, the same feedback gains that were used to generate the solution in Fig. 5 will now be used to generate a solution for a different range ( $L = 6000$  n mile, roughly the distance between New York and Tokyo), and a different wind shear profile ( $V_{ws1} = -0.1$  kn/n mile,  $V_{ws2} = 0.1$  kn/n mile, and  $V_{ws3} = 0.1$  kn/n mile). The nondimensional feedback gains remain unchanged, but the nondimensional perturbation values must be scaled according to Eqs. (33–35). For example, the nondimensional perturbation of the wind shear at the origin used to generate Fig. 5 was given by  $\eta_{ws} = (0.4 \text{ kn/n mile})(2500 \text{ n mile}/480 \text{ kn})$ , but now will be given by  $\eta_{ws} = (0.1 \text{ kn/n mile})(6000 \text{ n mile}/480 \text{ kn})$ .

The new simulation demonstrates the same near-optimal performance as in the preceding example but with a time savings of almost one-half hour (3.4% of the optimal flight time) in this case (Fig. 7).

Practical Applications

The NOC algorithm may form the basis for practical horizontal-path wind-optimal routing for long-haul flights. Airlines currently employ vertical-path optimization schemes to determine optimal climb/cruise/descent profiles subject to a wide variety of airspace constraints. Vertical-path optimization is mainly a function of aircraft aerodynamic and engine performance, and vertical wind gradients, whereas horizontal-path optimization is a function of horizontal wind gradients. These two optimization goals are only weakly coupled. For long haul flights, vertical-path optimization results in climb and descent segments and long, constant altitude segments, and it is intended that NOC wind-optimal routing would be applied to the constant altitude segments of these flights. For flights with significant altitude variations, for example, optimal step-climb profiles, the NOC algorithm presented could be extended to include terms for vertical wind gradients in the same way that horizontal wind gradient terms have been included. In principle, algorithmic coupling of the vertical performance optimization and the horizontal wind optimization would be required to achieve optimum performance, but this would defeat the computational simplicity achieved by the NOC algorithm. A final step in the optimization process would be to satisfy airspace constraints such as jet route constraints, special-use airspace, and bad weather areas.

The use of NOC for wind-optimal routing would be similar for either onboard flight management systems or ground-based automation systems such as the Center-Terminal Radar Approach Control Automation System.<sup>7</sup> Note that ground-based automation might be used by air traffic control (ATC), airline operations centers, or both. Currently, near real-time wind data for use in optimization can be

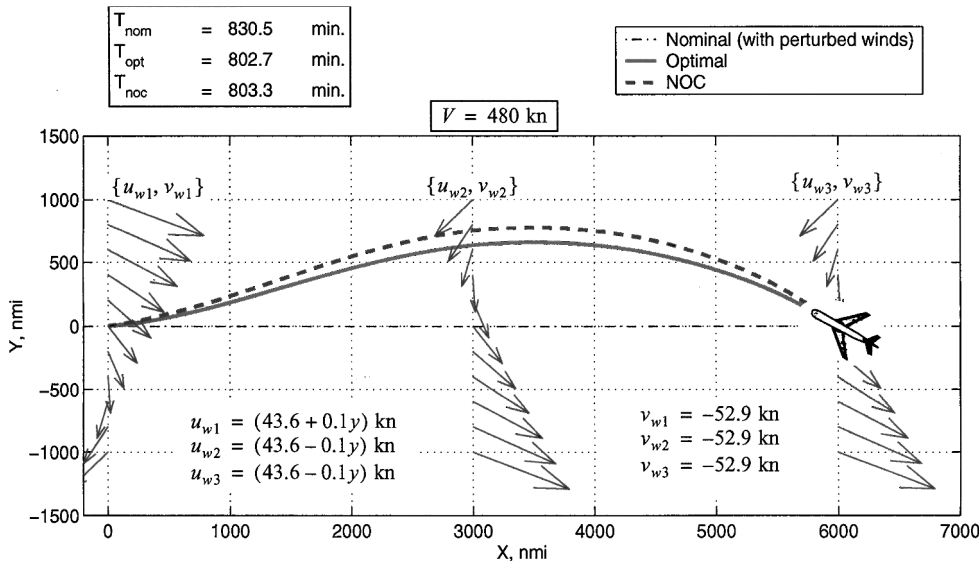


Fig. 7 Similar solution can be generated from the nondimensional solution by changing the scale factors associated with speed and distance and by modifying the perturbation values accordingly.

**Table 1** Nominal and perturbed values of wind and wind shear parameters

Simulation	$V_{ws1}$ , kn/n mile	$V_{ws2}$ , kn/n mile	$V_{ws3}$ , kn/n mile	$u_{w1}$ , kn	$u_{w2}$ , kn	$u_{w3}$ , kn	$v_{w1}$ , kn	$v_{w2}$ , kn	$v_{w3}$ , kn
Nominal	0	0	0	39.9	39.9	39.9	12.5	12.5	12.5
Perturbed	0.4	0	-0.4	43.6	43.6	43.6	-52.9	-52.9	-52.9

obtained once per hour from a continental-scale gridded wind model like the rapid update cycle (RUC),<sup>8</sup> or at a higher update rate (as often as once every 5 min) from a system like the Integrated Terminal Weather System (ITWS),<sup>6,9</sup> which blends real-time aircraft wind reports and terminal weather radar data into the base RUC data. To illustrate how the algorithm might be applied in the current-day ATC environment, the steps to be used for a ground-based automation system are outlined as follows.

1) Precompute and store tables of nondimensional NOC guidance-loop feedback gains for a small set of typical cases of wind and wind shear.

2) Retrieve real-time wind measurement updates as often as possible/practical (1-h update for RUC, 5–15 min update for ITWS).

3) Determine optimal vertical flight profile based on current airspace conditions and aircraft schedules.

4) For a given set of initial and final way points, perform coordinate transformations to match the flight-direction-aligned coordinate system employed during NOC feedback gain computation.

5) For a given airspeed and flight range, dimensionalize and apply the NOC feedback gains in fast-time simulation mode to determine wind-optimal trajectory clearances.

6) Fit the wind-optimal trajectory clearances as closely as possible with existing way points and routes as required by airspace constraints (ATC route constraints, special-use airspace, weather fronts, etc.).

7) Uplink wind-optimal clearances to the aircraft via data link.

## Conclusions

The NOC method has been extended by augmenting a dynamic model with additional states to account for parameter perturbations. This approach to incorporating parameter perturbations has the advantage that it does not require any modifications to NOC solution techniques, and time-varying parameter perturbations are handled just as easily as bias parameter perturbations. Simulations of the time-optimal aircraft trajectory problem for a bias parameter perturbation have been presented to demonstrate the state-augmentation method. In this case, NOC with an augmented parameter state produced trajectory solutions that were nearly identical to the optimal trajectories. The time savings resulting from NOC wind optimization was about 4% for the 2500-nmile, range simulation example.

To show how the NOC technique can be used to compute minimum-time trajectories in general wind fields for a wide range of aircraft flight conditions, a nondimensional form of the NOC solution was derived, and piecewise linear wind and wind shear terms were included. A simulation was presented to demonstrate NOC performance in a general wind field and a range of 2500 n mile, and a second simulation was performed to demonstrate that the same NOC feedback gains could be used to generate a near-optimal solution for an aircraft with a much greater range (6000 n mile). The time savings in these simulations were 5 and 27 min, respectively.

Finally, the optimal trajectory guidance of commercial aircraft in general wind fields by both onboard and ground-based systems has been suggested as an application that could benefit from NOC with augmented parameter states. Operational scenarios for both onboard and ground-based trajectory optimization systems have been presented.

## References

- <sup>1</sup>Bryson, A. E., Jr., and Ho, Y. C., *Applied Optimal Control: Optimization, Estimation and Control*, rev., Hemisphere, New York, 1975, pp. 77–80.
- <sup>2</sup>Bryson, A. E., Jr., *Dynamic Optimization*, Addison-Wesley, Menlo Park, CA, 1999, pp. 295–297, 318–323.
- <sup>3</sup>Lee, A. Y., and Bryson, A. E., Jr., “Neighbouring Extremals of Dynamic Optimization Problems with Parameter Variations,” *Optimal Control Applications and Methods*, Vol. 10, No. 1, 1989, pp. 39–52.
- <sup>4</sup>Speyer, J. L., “Robust Perturbation Guidance for the Advanced Launch System,” *Proceedings of the 1989 American Control Conference*, IEEE Publications, Piscataway, NJ, 1989, pp. 2489–2494.
- <sup>5</sup>Jardin, M. R., and Erzberger, H., “Atmospheric Data Acquisition and Interpolation for Enhanced Trajectory-Prediction Accuracy in the Center-TRACON Automation System,” AIAA Paper 96-0271, Jan. 1996.
- <sup>6</sup>Cole, R. E., Green, S. M., and Jardin, M. R., “Improving RUC-1 Wind Estimates by Incorporating Near Real-Time Aircraft Reports,” *Weather and Forecasting*, Vol. 15, No. 4, pp. 447–460.
- <sup>7</sup>Erzberger, H., Davis, T. J., and Green, S., “Design of Center-TRACON Automation System,” CP-538, AGARD, May 1993, pp. 11-1–11-12.
- <sup>8</sup>Benjamin, S. G., Brundage, K. J., Miller, P. A., Smith, T. L., Grell, G. A., Kim, D., Brown, J. M., Schlatter, T. W., and Morone, L. L., “The Rapid Update Cycle at NMC,” *Preprints, Tenth Conference on Numerical Weather Prediction*, American Meteorological Society, Boston, MA, 1994, pp. 566–568.
- <sup>9</sup>Cole, R. E., and Wilson, F. W., “ITWS Gridded Winds Product,” *Sixth Conference on Aviation Weather Systems*, American Meteorological Society, Boston, MA, 1994, pp. 384–389.